



HAL
open science

Battery-free Bluetooth Low Energy Wireless Sensor Powered by Radiative Wireless Power Transfer

Alassane Sidibe, Gael Loubet, Alexandru Takacs, Lamoussa Sanogo, Daniela
Dragomirescu

► **To cite this version:**

Alassane Sidibe, Gael Loubet, Alexandru Takacs, Lamoussa Sanogo, Daniela Dragomirescu. Battery-free Bluetooth Low Energy Wireless Sensor Powered by Radiative Wireless Power Transfer. NewCAS 2023, IEEE, Jun 2023, Edinburg,, United Kingdom. 10.1109/NEWCAS57931.2023.10198088 . hal-04157047

HAL Id: hal-04157047

<https://laas.hal.science/hal-04157047>

Submitted on 10 Jul 2023

HAL is a multi-disciplinary open access archive for the deposit and dissemination of scientific research documents, whether they are published or not. The documents may come from teaching and research institutions in France or abroad, or from public or private research centers.

L'archive ouverte pluridisciplinaire **HAL**, est destinée au dépôt et à la diffusion de documents scientifiques de niveau recherche, publiés ou non, émanant des établissements d'enseignement et de recherche français ou étrangers, des laboratoires publics ou privés.

Battery-free Bluetooth Low Energy Wireless Sensor Powered by Radiative Wireless Power Transfer

Alassane Sidibe¹, Gaël Loubet², Alexandru Takacs³, Lamoussa Sanogo⁴, Daniela Dragomirescu⁵

LAAS-CNRS, Université de Toulouse, INSA, UPS, CNRS, 31400, Toulouse, France

¹alassane.sidibe@laas.fr, ²gael.loubet@laas.fr, ³alexandru.takacs@laas.fr, ⁴lamoussa.sanogo@laas.fr,

⁵daniela.dragomirescu@laas.fr

Abstract—This paper addresses the design and the characterization of a battery-free Bluetooth Low Energy (BLE) wireless sensor node powered by radiative wireless power transfer. The battery-free sensors node, as part of a wireless meshed network, is optimized and is able to perform physical measurements (temperature and humidity) and share these measured data over the Internet through the wireless network. It operates by using a standard capacitor of 220 μF as a storage element and is remotely powered by a dedicated RF source using a radiative wireless power transfer. The main task initialization, sensing and broadcasting the measured data by using a BLE protocol requires only 1.2 mJ of energy per task. More the periodicity of physical measurements can be roughly controlled by controlling the radiated power of the RF source.

Keywords—Battery-free Sensors, Wireless Power Transfer (WPT), Power Management, Bluetooth Low Energy (BLE)

I. INTRODUCTION

The deployment at large scale of Internet of Things (IoT) solutions for various applications including but not limited to Structural Health Monitoring (SHM), requires the use of wireless Sensor Nodes (SN). In most cases, these SN are powered by batteries. The major drawbacks of using batteries are related to limited lifetime, environmental and maintenance issues mainly when SN are inaccessible (e.g. SN embedded in concrete structures, walls, etc.). One solution to overcome these drawbacks is to use passive sensors (e.g. passive RFID [1], sensors interrogated by radar techniques [2], etc.) or active battery-free SN (BFSN). In the case of BFSN, the battery is replaced by an energy storage element (e.g. supercapacitor, capacitor, etc.) that can be recharged by energy harvesting or Wireless Power Transfer (WPT) techniques [3], [4], [5]. This paper addresses the design, implementation, and characterization of a wireless BFSN using Bluetooth Low Energy (BLE) [5]. The design methodology is presented in section II and section III deals with the architecture of BFSN. Section IV presents the characterization and the experimental results obtained for the wireless BLE BFSN.

II. DESIGN METHODOLOGY

An efficient design of wireless sensors network including battery-free wireless sensors involves several key points that have to be simultaneously addressed at the network and sensor levels: (i) optimization of the network topology for maximizing the energy collected by the battery-free sensors, and for minimizing the number of dedicated Wireless Power Transmission sources, but also the total power radiated by those sources; (ii) selection of an optimal solution for implementing the Simultaneous Wireless Information and Power Transfer (SWIPT); (iii) minimization of the DC consumption of the battery-free wireless sensors at hardware and software levels; and (iv) optimization of the power

management strategy and reduction of the leakage of the energy storage element (e.g. supercapacitor, capacitor, etc.).

Based on our selected scenario (SHM and the use of radiative WPT from a dedicated RF source [6]) we targeted a BFSN that can measure physical data such as the temperature, the humidity and the material resistivity inside of civil engineering structures (e.g. concrete beams, walls, bricks, etc.) with a minimal energy consumption and transfer these physical data worldwide over the Internet. It is obvious that only one wireless BFSN will not be able to satisfy the design requirements presented before. A mesh network has been designed as shown in Fig. 1. The network consists of BFSN connected to Communicating Nodes (CN). In order to save energy on the BFSN side, only an uplink communication path has been established between the SN and CN, and the Internet connection is only available at the CN level (CN are supposed to be not impacted by energy availability and equipped with a reliable energy source).

We chose the BLE as wireless technology. BLE seems to be a good trade-off in terms of availability (almost all of today's computers and smartphones are BLE-equipped), energy consumption, and communication range.

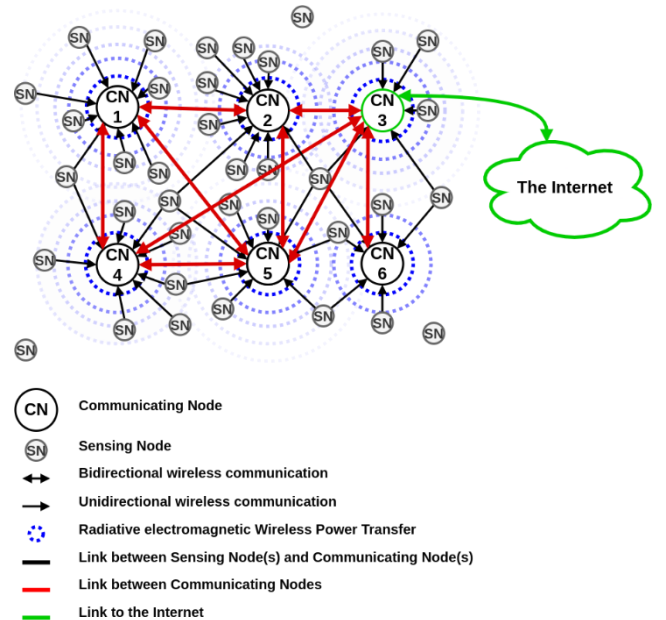


Fig. 1. Topology of the mesh network including battery-free SN.

III. BATTERY-FREE SENSOR NODE ARCHITECTURE

The BFSN architecture has been optimized at the hardware and software level in order to be: (i) battery-free, low power, cold-start compatible (i.e. BFSN can start-up by charging the

storage element – e.g. capacitor – from its empty state) and remotely powered by using at radiative WPT technique. The topology of the BFSN is detailed in Fig. 2 and the detailed electrical schema as well as a photo of the manufactured prototype are depicted in Fig. 4. BFSN is composed of a rectifier (topology represented in Fig. 3) operating in ISM 868 MHz frequency band, a power management unit PMU (AEM30940 [7]), a BLE system-on-chip (QN9080 [8]) a temperature (T) and humidity (H) low power active sensor (HDC2080 [9]) and analog circuitry to drive an external resistivity sensor (this part is not addressed by this paper) able to monitor corrosion issues in reinforced concrete structures.

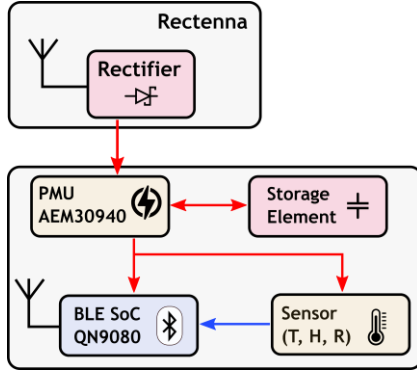


Fig. 2. Bloc diagram of the battery-free SN

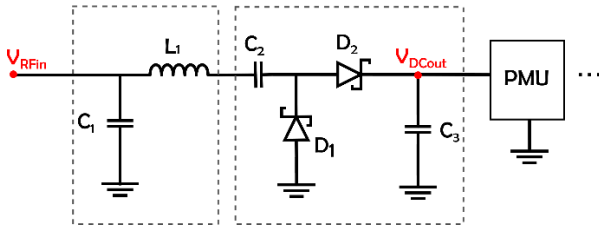


Fig. 3. Topology of the RF rectifier operating in the ISM 868 frequency band

The rectifier represented in Fig. 3 consists of an LC matching network ($L_1 = 33$ nH type LQW15AN33NG00 and $C_1 = 4$ pF, type GRM1551X1H4R0CA01D), a series pair Schottky diode (SMS7630-005LF) [10] and a shunt capacitor used as part of a low pass-filter with load represented by the input impedance of the PMU. The BFSN can be also powered from an external DC source. Wireless data communication is enabled by an ultra-low power BLE SOC (QN9080 SoC [7]), and a conventional meandered inverted-F antenna operating at 2.45 GHz. To configure the PMU with the provided configuration tools from the manufacturer, the total power required by the sensors and transceiver has been evaluated based on the typical current consumption profile (represented in Fig. 5) of the BLE BFSN during sensing (temperature and humidity measurements) and broadcasting. The sensing data (temperature and humidity) are sent to the CN over 4 advertising cycles. On each advertising event, the same data frame is broadcasted over BLE channels n° 37, 38 and 39. This high redundancy on the BLE SN side minimizes the probability of errors caused by potential interferences mainly with Wi-Fi transmitters operating roughly in the same frequency band. As shown in Fig. 5, all the tasks (initialization, sensing, broadcasting and stop advertising) are performed in approximately 1.3 s. The implemented power management algorithm involves the use of two voltage levels

at the input of the storage element C_{store} (a standard capacitor of 220 μ F, type EEEFK0J221P) $V_{C_{store} MAX} = 4,23$ V, and, $V_{C_{store} min} = 1,94$ V. Note that C_{store} was dimensioned by considering the DC consumption of the analog circuitry to drive an external resistivity sensor (this part is not addressed by this paper). Without this supplementary DC consumption, the capacitance value of the storage element can be reduced to 100 μ F.

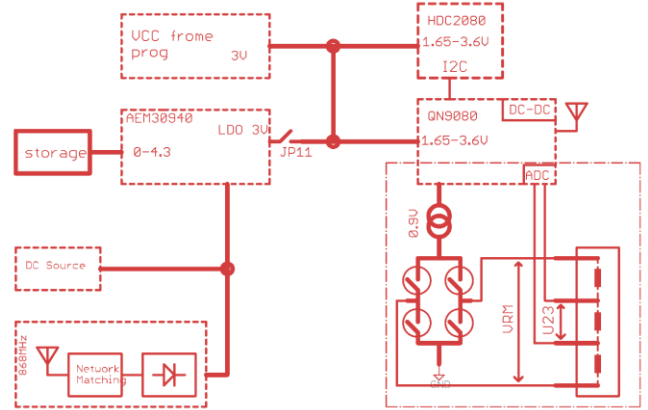


Fig. 4. Electrical schema of the BFSN and a photo of the manufactured of battery-free SN prototype including a flexible antenna manufactured on PET substrate operating in ISM 868 MHz frequency band.

IV. EXPERIMENTAL RESULTS

For characterization purposes, the BFSN was tested: (i) powered directly from a RF signal generator (in this case the RF power is directly injected at the input of the rectifier as shown in Fig. 6 a) and no WPT/868 MHz antenna was used), and, (ii) in an anechoic chamber (setup represented in Fig. 6. b). The experimental setup of Fig. 6 b) is composed of signal generator connected to a homemade patch antenna (maximum gain of +9.4 dBi at 868 MHz) operating as a RF source and a CN composed of BLE QN9080 development kit [11] connected to a laptop that enables to receive the transmitted data by the BFSN. By using this CN is possible to receive the sensing data (temperature and humidity) to share the data over the Internet and to measure the first charge (start) duration and recharge periodicity of the storage capacitor. The distance between the RF source and BFSN is two meters and the computed free space losses at this distance are around +37.23 dB at 868 MHz. The first charge duration corresponds to the duration required for the first measurement (in this case we have a so-named 'cold-start' – the initial voltage across the storage capacitor is 0 V – and it is charged

up to $V_{C_store\ MAX} = 4,23\text{ V}$). During the sensing and data broadcasting the voltage across the capacitor draws to $V_{C_store\ min} = 1.94\text{ V}$ and then the BFSN switch to a deep-sleep mode and the capacitor is recharged again by the DC energy provided by the rectifier through PMU unit. The recharge periodicity of the energy storage element (capacitor) corresponds with the periodicity of sensing and broadcasting and can be roughly controlled by controlling the Effective Isotropic Radiated Power (EIRP) of the dedicated RF source that is regulated at maximum 2 W in the ISM 868 MHz frequency band. The RF source is driven by the CNs and can be integrated/collocated or not with the RF source.

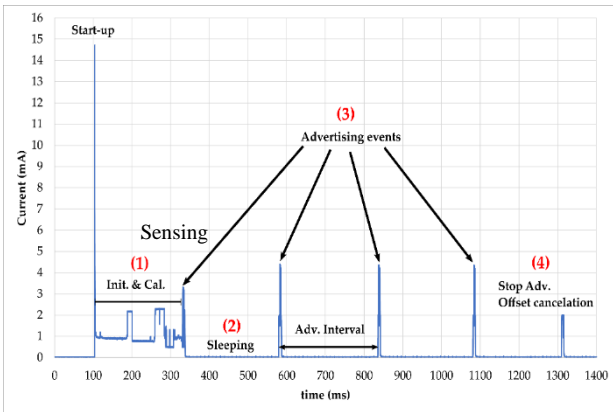


Fig. 5. Dc current consumption profile of the BLE SN during sensing and broadcasting obtained with the power measurement tool of MCUXpresso IDE software.

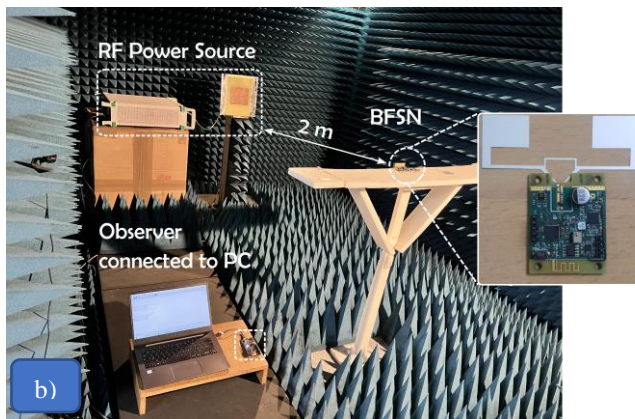


Fig. 6. Experimental setup to mesure a BLE BFSN (mode boadcasting/advertising) : (a) when it is powered by the RF energy delivered from a RF generator, and, (b) in a anechoic chamber by using a radiative WPT technique, a dedicated RF source, and a BLE card (connected to a laptop) configured as observer.

The measured charge durations (same as sensing and broadcasting) obtained by using the experimental setup of Fig 6 a) are represented in Fig. 7. The energy consumption is around of 1.4 mJ for the first charge (charging the capacitor

from 0 V) and around of 1.2 mJ for the second charge/recharges (periodically charging from $V_{C_store\ min} = 1.94\text{ V}$ to $V_{C_store\ MAX} = 4,23\text{ V}$). However, it should be noted that these results do not reveal the true performances of the BFSN. The developed board does not have a dedicated RF connector to be power supplied. It was therefore necessary to use a feeding technique through an SMA transition to crocodile clips. Since this transition is not suitable, it will induce losses and the power delivered by the power generator is not that at the rectifier input. Thus, we had to better characterize our prototype with an antenna. The experimental results obtained by using the setup represented in Fig 6. b) are summarized in Table I. As expected the first start charge and the recharging are function of the EIRP of the RF source and ranging from 54 s (EIRP = +32.7 dBm) to 1073 s (EIRP = +24.7 dBm) for the first charge and from 27 s (EIRP = +32.7 dBm) to 501 s (EIRP = +24.7 dBm) for the recharge duration. The experimental results depicted in Fig. 7 was obtained by using a high-impedance oscilloscope connected at the storage capacitor ports while the results of Table I were obtained by using software measurements performed at the CN level.

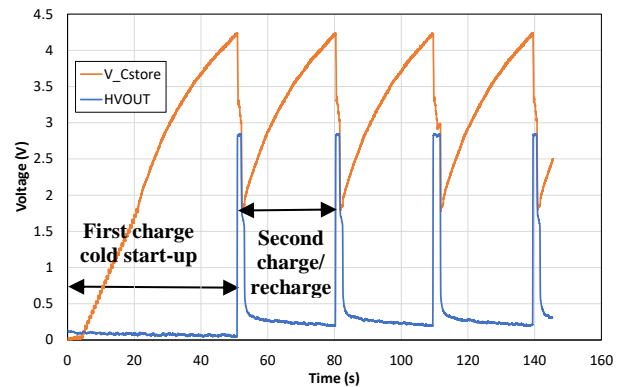


Fig. 7. Measured voltage at the input port of the storage capacitor (V_{Cstore}) and at the output of the power management unit ($HVOUT$) as function of time. Experimental results obtained by using the setup represented in Fig 6 b) for a RF power at +6 dBm delivered by the RF generator and injected to the rectifier input of the BFSN.

TABLE I. CHARGING DURATIONS (S) AS FUNTION OF THE RF POWER

P_{TX} (dBm)	EIRP (dBm)	P_{RX} (dBm)	1 st charge (s)	Recharge (s)
+24	32.7	-3.33	54	27
+22	30.7	-5.33	105	49.83
+20	28.7	-7.33	200	96
+18	26.7	-9.33	420	206.25
+16	24.7	-11.33	1073	501.33

In order to implement the simultaneous wireless information and power transfer we used a frequency multiplexing technique and two antennas: one for WPT operating at 868 MHz in receiving mode (from RF source to BFSN) and one for data sending (from BFSN to CN) operating at 2.45 GHz. BLE battery-free solutions were also proposed in [4] (required storage capacitor of 330 μF and uses a BLE SoC provided by STMicroelectronics) for asset tracking modules. By using the solution proposed in this paper we need lower energy and consequently we need a capacitor with a lower capacitance but the selected application in [4] is quite different from our application for a fair comparison.

V. CONCLUSION

An innovative architecture of a wireless BFSN was presented in this paper and the experimental results confirm that by using a standard capacitor of only 220 μF and an energy of 1.2 mJ approximately the BFSN can measure the temperature and the humidity and broadcast data over the Internet thanks to the use of a dedicated mesh sensor network.

Also, the periodicity of the charging of the storage capacitor can be roughly controlled by tuning the EIRP of the RF source.

REFERENCES

- [1] Amin Rida, Li Yang, Manos Tentzeris, RFID-Enabled Sensor Design and Applications, Artech House Publishers, 2010
- [2] D. Henry, T. Marchal, J. Philippe, P. Pons and H. Aubert, "Classification of Radar Echoes for Identification and Remote Reading of Chipless Millimeter-Wave Sensors," in IEEE Transactions on Microwave Theory and Techniques, vol. 69, no. 1, pp. 926-937, Jan. 2021
- [3] La Rosa R, Livreri P, Trigona C, Di Donato L, Sorbello G. Strategies and Techniques for Powering Wireless Sensor Nodes through Energy Harvesting and Wireless Power Transfer. *Sensors* (Basel). 2019 Jun 12;19(12)
- [4] La Rosa, R.; Dehollain, C.; Livreri, P. Advanced Monitoring Systems Based on Battery-Less Asset Tracking Modules Energized through RF Wireless Power Transfer. *Sensors* **2020**, *20*, 3020
- [5] Bluetooth Technology Overview Available online: <https://www.bluetooth.com/learn-about-bluetooth/tech-overview/> (accessed on 6 December 2021).
- [6] Not showed here for blind review
- [7] AEM20940 RF Energy Harvesting | Radio Frequency Harvesting Available online: <https://e-peas.com/product/aem30940/>
- [8] QN908x: Ultra-Low-Power Bluetooth Low Energy System on Chip (SoC) Solution | NXP Semiconductors Available online: <https://www.nxp.com/products/wireless/bluetooth-low-energy/qn908x-ultra-low-power-bluetooth-low-energy-system-on-chip-solution:QN9080>.
- [9] <https://www.ti.com/product/HDC2080>
- [10] <https://store.skyworksinc.com/products/detail/sms76300051f-skyworks-solutions-inc/113182/>
- [11] QN9080SIP Development Kit Available online: <https://www.nxp.com/design/development-boards/freedom-development-boards/wireless-connectivity/a-highly-extensible-platform-for-application-development-of-qn9080sip:QN9080SIP-DK> (accessed on 14 February 2022)